Biochemical and Biophysical Research Communications 422 (2012) 97–102

Contents lists available at SciVerse ScienceDirect

Biochemical and Biophysical Research Communications

journal homepage: www.elsevier.com/locate/ybbrc

Rapid degradation kinetics of amyloid fibrils under mild conditions by an archaeal chaperonin

Dmitry Kurouski [a], Haibin Luo [b], Valentin Sereda [a], Frank T. Robb [b], Igor K. Lednev [a,*]

[a] University at Albany, State University of New York, 1400 Washington Avenue, Albany, NY 12222, USA
[b] Institute of Marine and Environmental Technology, Department of Microbiology and Immunology, University of Maryland School of Medicine, 685 West Baltimore Street, Baltimore, MD 21201, USA

ARTICLE INFO

Article history:
Received 13 April 2012
Available online 30 April 2012

Keywords:
Hyperthermophile
Archaea
Cpn
Amyloid fibrils
Insulin
Fibril degradation

ABSTRACT

Amyloid depositions containing exceptionally stable β-sheet rich protein aggregates, called fibrils are associated with prevalent and incurable neurodegenerative diseases. Chaperones are proteins that facilitate protein folding in both eukaryotes and prokaryotes. We found that a cold-adapted mutant ATP-dependant chaperonins (Hsp60) from a hyperthermophilic archaeon binds to and fragments insulin fibrils very rapidly with local targeted entry points. Individual fragments swell and the fibrillar β-sheet is quickly transformed into a mix of α-helical and unordered protein structures. After further incubation, the fragments coalesced, forming large amorphous aggregates with poly-disperse topologies. This finding represents a new approach to the disassembly of refractory protein aggregates under physiological conditions.

1. Introduction

Amyloid depositions, containing exceptionally stable β-sheet rich protein aggregates called fibrils, are associated with several debilitating neurodegenerative diseases. The role of amyloid fibrils in these maladies remains elusive. A large body of evidence suggests that amyloid fibrils are toxic species, which cause misfolding and aggregation of native functional proteins. According to a current hypothesis, amyloid fibrils are warehouses of misfolded proteins, that entrain toxic species that, left unchecked, would cause neurodegenerative diseases [1]. Consequently, therapeutic and pharmaceutical strategies target the appearance and possibly deconstruction of amyloid fibrils. The latter strategy is difficult to implement *in vivo* since the extreme stability of most amyloid structures dictates the use of harsh conditions that are not clinically applicable. Several small molecules have been reported to prevent monomeric protein aggregation during the initial stages of fibrillation [2,3] . Some of these molecules are purported to arrest a protein aggregation by competitive binding to the fibril oligomers. At the same time, mature amyloid fibrils resist small molecule attack. Harsh dispersion conditions, such as a strongly alkaline medium, [4] low temperature, and high pressure, [5] are required to disintegrate mature fibrils formed from full-length proteins. Recent findings supporting the suggestion that pre-amyloid species are more toxic than the amyloid deposits themselves. For example, amyloid β (Aβ) dimers and oligomers have higher toxicity than fibrils, during extracellular delivery to cell lines or *in vivo* when injected into rat brain [6,7] . Moreover, fibril precursors, such as proto-filaments and proto-fibrils of insulin have higher toxicity than mature fibrils [8]. If this is true, intra and extra cellular conversion of the misfolded proteins and their oligomers into highly ordered amyloid forms may in fact diminish the level of these toxic species and therefore be protective.

In this study, we address the factors affecting the dispersion of amyloid fibrils formed from human insulin. A common clinical condition, known as injection amyloidosis, is observed when a high local concentration of insulin causes its under-skin aggregation in the form of fibrils [9,10] . Insulin is a very well-studied peptide hormone that has two polypeptide chains linked by two inter-chain and one intra-chain disulfide bonds. In native form, insulin has mainly α-helical secondary structure. Upon aggregation into fibrils, native insulin undergoes structural change into β-sheet rich conformations. Often, insulin *in vitro* fibrillization results in the formation of morphologically heterogeneous fibrils, a phenomenon known as fibril polymorphism [11].

The interactions of heat shock proteins with amyloid fibrils have drawn significant attention in recently years. However, most of these studies focus on one group of heat shock proteins with small molecular mass, so called small heat shock proteins [12,13]. Many small heat shock proteins have been reported to disassemble fibrils or prevent the fibrillation process *in vitro* [14]. For example, small

Abbreviations: Pf, *Pyrococcus furiosus*; Hsp60, heat shock protein; Cpn, chaperonin; CD, circular dichroism.

* Corresponding author.
E-mail address: ilednev@albany.edu (I.K. Lednev).

0006-291X/$ - see front matter © 2012 Elsevier Inc. All rights reserved.
http://dx.doi.org/10.1016/j.bbrc.2012.04.113

heat shock protein 104 from yeast disassembled mature prion fibrils *in vitro* [15,16]. Hsp104 changes the secondary structure of PrP fibrils from β-sheet to a random coil [17]. MTT tests confirmed that Hsp104 treated PrP maintained the same level of toxicity as untreated protein fibrils [18]. Human small heat shock proteins have been found to inhibit the assembly and elongation of alpha-synuclein amyloid fibrils [17]. Several other heat shock proteins have been reported to show a similar impact on fibrils [19]. For instance, heat shock protein 70 and Hsp90 modulate the assembly of alpha-synuclein amyloid fibrils [20–23]. Human heat shock protein 60 (also known as Chaperonin) cooperates with heat shock protein 70 preventing huntingtin protein from fibrillation [19].

Chaperonins are divided into Group I, represented by GroEL found in all bacteria, mitochondria and chloroplasts, and Group II complexes, occurring in eukaryotes and archaea. Group I chaperonins require a co-chaperone, GroES, to facilitate protein folding, however group II chaperonins can function without a co-chaperone. Functional double-ring complexes of group II chaperonins usually consist of two or more different subunits [24,25]. The chaperonin complex from *Pyrococcus furiosus* (Pf), in common with most hyperthermophiles [26], is composed of identical subunits and therefore is minimally complex [24,27]. Pf chaperonin is exceptionally stable, but has very limited activity below 50 °C. We have recently demonstrated that a hyperstable chaperonin with mutations that increase flexibility of the carboxyl terminus is highly active at relatively low temperatures [28]. Here we report a comprehensive investigation of the kinetic mechanism of insulin fibril deconstruction by this mutated Cpn.

2. Materials and methods

2.1. Insulin fibril preparation

Bovine insulin (60 mg/ml), purchased from Sigma–Aldrich, St. Louis, MO, was dissolved in water with a final pH adjusted by concentrated HCl to pH 2.5. The protein solution was incubated at 70 °C for 2 h. The insulin fibrillation process was terminated by reducing the temperature to ~25 °C. Non-aggregated protein was removed by a sample centrifugation at 14.000*g* for 20 min. After a supernatant was removed, a gelatinous phase, dominated by mature fibrils, was re-dispersed in HCl solution with pH 2.5. The centrifugation–redispersion procedure was repeated twice.

2.2. Chaperonin preparation

Pf Cpn was cloned and expressed as previously reported [24,28] . The supernatant extracts were heated at 70 °C for 30 min, and then they were purified to homogeneity by two steps of anion exchange: HiTrap™ Q HP cartridge from Biorad (Hercules, CA) and Bio-Scale™ macro-prep high Q cartridge from GE healthcare (Uppsala, Sweden).

2.3. Chaperonin-fibril reaction

Insulin fibrils were mixed with Cpn (0.05 mg/ml) in 20 mM sodium acetate buffer, pH 6.0 with 2 or 200 mM ATP. Mg ions, essential for Cpn activity, were added to the buffer together with sodium chloride to the final concentrations 1 and 50 mM, respectively.

2.4. Atomic force microscopy (AFM)

An aliquot of the analyzed solution was re-suspended in sodium acetate buffer, pH 6.0 with a 1:400 dilution factor (V/V). A drop of this solution was placed onto freshly cleaved mica and incubated for 2 min followed by removing of the solution excess. Finally, mica surface was dried under a nitrogen flow. AFM scanning was performed immediately in AC tapping mode using MFP-3D™ Bio Asylum Research microscope (Asylum Research, CA, USA) with Olympus AC160 tips.

2.5. Scanning electron microscopy (SEM)

For each sample 20 μL of analyzed solution were diluted in 1:400 ratio by distilled water and deposited on a 200-mesh copper grid. Staining with 1% uranyl acetate was performed in 10 min after the deposition. Samples were imaged on Zeiss Gemini Ultra 55 SEM (Oberkochen, Germany) in InLense mode with 5 kV EHT.

2.6. Far-UV CD spectroscopy

Far-UV CD (190–250 nm) spectra were measured using a JASCO J-810 (Jasco, Japan) spectropolarimeter at room temperature. For protein concentrations of ~1 mg/ml, a 0.02 cm path length cell was used. The CD spectra were acquired with 100 nm/min scan speed at 1 nm step and 2.0 nm bandwidth. Five spectra were accumulated and averaged for each sample. Protein secondary structure composition was evaluated using CCAplus software package. Four principal protein secondary structure components from CDPro package were taken to de-convolute the analyzed CD spectrum.

2.7. Thioflavin T (ThT) fluorescence assay

ThT fluorescence assays were performed on Fluorolog spectrofluorometer (HORIBA Jobin Yvone, Edison, NJ) at room temperature. The sample aliquot of 20 μL was mixed with 3 ml of Thioflavin T (25 μM, Sigma–Aldrich, St. Louis, MO) in 10-mM Phosphate buffer (pH 7.4). ThT emission spectra were recorded between 465 and 550 nm at 450 nm excitation using a 1 × 1 cm rectangular cell. The solution was stirred using a magnetic bar for several minutes before fluorescence measurements. The total of three spectra were measured for each sample and then averaged.

3. Results and discussion

3.1. Chaperonins modify and fragment insulin fibrils

Insulin fibrils prepared according to the literature procedure are shown in Fig. 1A and E. They conformed to the shape and size of 25 nm in width, around 8 nm in height (thickness) and with a variable length from 100 nm up to a several microns [11]. Fibrils were centrifuged and re-dispersed in pH 6.0, 20 mM sodium acetate buffer in the presence of Cpn (0.05 mg/ml) and ATP (2 mM) at 37 °C. The kinetics of fibril transformation caused by the Cpn activity were probed by AFM and SEM. Solution aliquots were taken 5 min, 15 min and 30 min after the reaction started. As evident from AFM images in Fig. 1B and C the insulin fibrils fragmented in a periodic pattern within 5 min of exposure to Cpn (Fig. 1B) and were swollen and foreshortened with significantly lower height (~6 nm) and width up to 200–400 nm (Fig. 1F and G, indicated by red arrows). The periodicity of initial processing by Cpn is reminiscent of the non-continuous formation of insulin fibrils reported by Knowles et al. [29]. Interestingly, white image features on the edges of the clamps mimic the outline of the original fibrils (Fig. 1B). Most likely they are fibrillar regions that were not melted by Cpn because the reaction was quickly terminated. These observations confirm that Cpn changes the fibril architecture, melting the fibril core and finally forming an amorphous protein mass from regular β-sheet structure. Microscopic observations of this phenomenon confirm the fibril swelling before fragmentation. A longer exposure of insulin fibrils to Cpn results in their

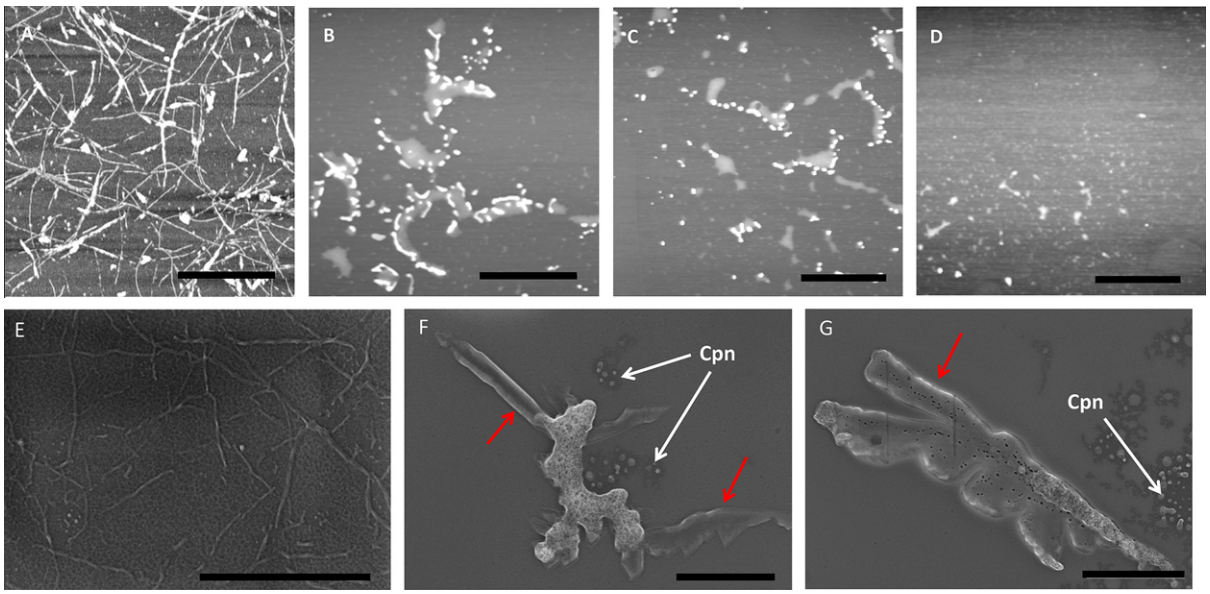

Fig. 1. Chaperonins degrade insulin fibrils. AFM (top row) and SEM (bottom row) images of insulin fibrils (A and E) before mixing with Cpn and 5 min (B), 15 min (C) and 30 min (D) after they were mixed with Cpn. Individual swollen fibrils (F and G, indicated by red arrows) have 200–250 nm in width and more than 1-μm in length and almost identical to the aggregates observed by AFM (top row, B). Cpn (marked with white arrows) were also evident in the reaction mixture. The scale bar is 1 μm. (For interpretation of the references to color in this figure legend, the reader is referred to the web version of this article.)

further fragmentation into smaller and smaller species with irregular shapes (Fig. 1C and D). These species coagulate during late stages, forming large amorphous aggregates.

Most of the fibril-shaped species disappear and predominantly amorphous objects form after 30-min of Cpn-fibril co-incubation (Fig. 1D). At later stages, these small amorphous species coagulate, forming large aggregates as discussed below. Small spherical particles (~30-nm width and ~12-nm height), which are evident on several AFM images (Fig. 1C and D), appear to be formed from fibrils and are likely not Cpn single particles which are 0.7-nm height (Supplementary Fig. 1) [30].

In fact, prolonged exposition of insulin fibrils without Cpn at the same experimental conditions (20-mM sodium acetate, pH 6.0, 2-mM ATP) at 37 °C, caused no changes in their morphology (Supplementary Fig. 2).

3.2. Effects of prolonged Cpn activity

SEM images a much larger sample area than AFM, providing a better characterization of heterogeneous samples. We utilized SEM for the characterization of products present after four hours of exposure to Cpn. Amorphous aggregates, which dominate SEM images in Fig. 2, are the result of coagulation of the swollen fibril fragments formed after 30 min incubation (Fig. 1D). Most aggregates have a spongy surface with distinct features of various sizes. The aggregates were no longer uniform in shape and size (in contrast to initial fibrils) and exhibited a complex morphology (Fig. 2A and B). Large amorphous species with no specific shape or size formed after several hours of chaperonin activity.

3.3. A fibril polymorph resistant to Cpn

While the majority of insulin fibrils fragment, swell and coagulate, forming spongy aggregates, a small proportion of fibril fragments retain their initial width and thickness after several hours of exposure to Cpn. SEM images in Fig. 2C show short fragments of intact, not swollen fibril fragments. Longer fragments with morphology resembling that of initial fibrils are also evident in the SEM image presented in Fig. 2D. We assume that this indicates the presence of a specific fibril polymorph(s), which is resistant to Cpn. The formation of several insulin fibril polymorphs under the same [31] and different [11] fibrillation conditions has been well documented.

In order to rule out the possibility that the intact fibril fragments remained after four hours of incubation because the Cpn activity was exhausted following ATP depletion, we performed the following experiment. The Cpn-substrate reaction is an equilibrium process, involving ATP hydrolysis to ADP and the release of phosphate. The accumulation of phosphate in solution could suppress the Cpn activity by product inhibition. We carried out two experiments to test this hypothesis. First, increasing the ATP concentration by 100 fold did not result in the degradation of the remaining intact fibril fragments. Secondly, the fibril-Cpn-ATP solution was centrifuged after a four hour incubation and the supernatant, containing small molecules, was decanted. The remaining material was washed with buffer and then re-dispersed in a fresh solution of Cpn and ATP (100 mM NaCl, 20 mM sodium acetate buffer, pH 6.0, 2 mM ATP and 1 mM Mg ions). Intact fibril fragments were again evident in the latter solution after four hours of incubation at 37 °C (data not shown). These two experiments confirmed that the remnant of intact fibril fragments differ from the bulk fibrils and are resistant to the chaperonin activity. Further study is required to understand the structural characteristics that render these fibrils resistant to chaperonins. Based on the literature available now, one can hypothesize that such fibrils (or their fragments) might have a hydrophilic surface preventing their interaction with chaperonins, which is typically based on hydrophobic contacts. Two observations support this hypothesis.

3.4. Protein secondary structure change during the insulin fibril transformation

It is well documented that β-sheet is the predominant protein conformation in insulin fibrils [11]. One may expect that such a dramatic deformation of fibril supramolecular architecture should be accomplished with extensive β-sheet degradation. In order to test the hypothesis we utilized thioflavinT (ThT) fluorescence assay, a universal analytical tool for fibrillar β-sheet detection

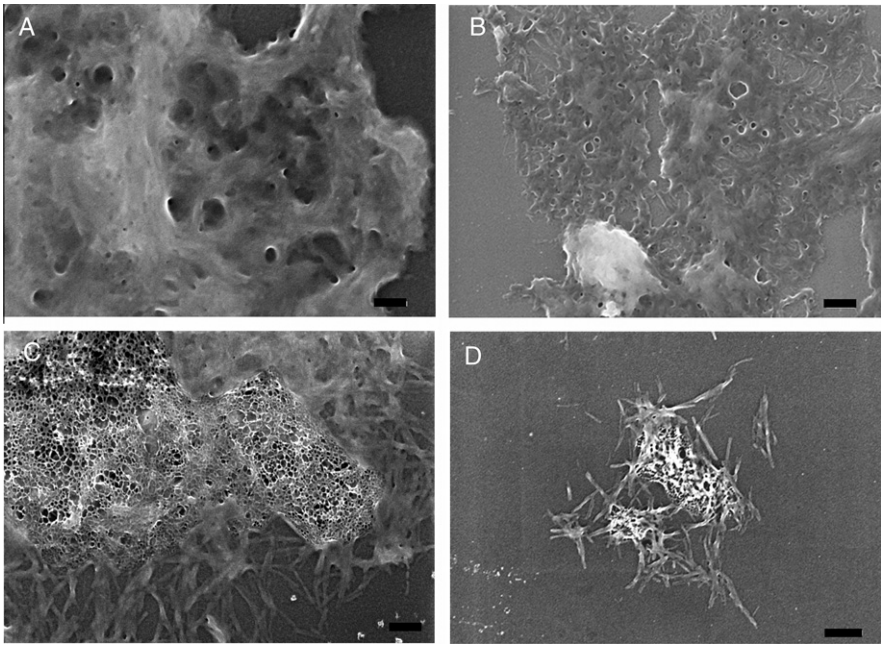

Fig. 2. Products of insulin fibril degradation. SEM images of amorphous aggregates (A–C) that were detected in the solution of insulin fibrils treated with chaperonins after 4 h. Some of them have porous surfaces (A and C), whereas a portion of them resemble a net of fibrillar fragments embedded in "melted" amorphous protein (B). Together with these amorphous aggregates some remaining fibrils were detected (D). These fibrils preserve the original morphology and remain relatively long and not swollen. Scale bar is 100 nm.

(Fig. 3A). A dramatic decrease in β-sheet content resulted from fibril co-incubation in the presence of Cpn-ATP. In fact, the Fibril-Cpn solution has a small residual ThT signal, which indicates that some β-sheet is resistant to dispersion. Control insulin fibrils incubated without Cpn in the presence of ATP at pH 6.0 show no significant decrease in β-sheet content (data not shown).

We applied circular dichroism (CD) to study changes in protein secondary structure accompanying the insulin fibril transformation induced by the Cpn. The far-UV CD spectrum of initial insulin fibrils indicates a dominating contribution of β-sheet (a trough at 217 nm, Fig. 3B). The spectrum changed significantly after addition of Cpn to the fibril solution and its incubation for four hours at 37 °C, indicating the appearance of α-helical and unordered protein structures and the decrease in β-sheet contribution. The CDPro database of the protein secondary structures was applied to the secondary structure composition based on CD spectra presented in Fig 3B. The initial fibrils were almost 100% β-sheet, whereas the chaperonin-treated fibrils were 14% α-helix, 19% unordered, 22% turns and 28% β-sheet.

3.5. Hypothetical mechanism

Scheme 1 represents a hypothetical mechanism of insulin fibril transformations caused by Cpn, which is consistent with all data presented above. At very early stages of fibril-Cpn co-incubation, the insulin fibrils became fragmented (reduced in length) and swollen, forming small gelatinous aggregates. After further incubation, these aggregates coagulated forming large amorphous aggregates with poly-dispersed topologies. The analysis of these transformations by CD spectroscopy and ThT assay indicated a substantial decrease in the fibril β-sheet content and the formation of α-helical and unordered protein structures.

It was also found that some insulin fibrils or fibril fragments are resistant to Cpn activity (colored features in Scheme 1). AFM images showed no Cpn single particles on these recalcitrant fibrils. We hypothesize that the surface of the Cpn-resistant fibril morphotype is more hydrophilic than that of fibrils attracting Cpn.

Kelly and co-workers [32] have recently discovered that a homogenized extract obtained from cells and tissue cultures can

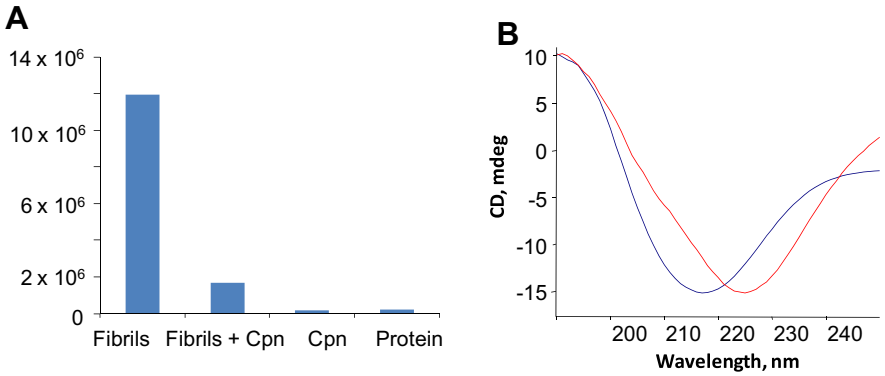

Fig. 3. Cpn cause a substantial depression of β-sheet and change fibril secondary structure. ThT (A) assay indicates a significant decrease of fibril β-sheet in (Fibril + Cpn) solution after 4 h of co-exposition comparing to (fibrils). Intact insulin (protein) and HSP60 chaperones (Cpn) show no ThT signal. CD spectra (B) of insulin fibrils (blue) and the same solution (red) after co-incubation with Cpn for four hours at 37 °C in the presence of 2 mM of ATP. (For interpretation of the references to color in this figure legend, the reader is referred to the web version of this article.)

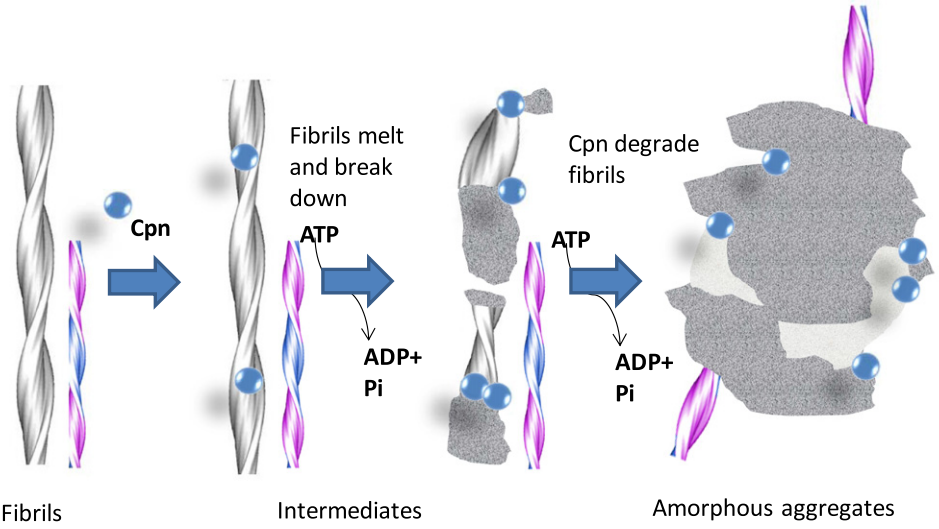

Scheme 1. Hypothetical mechanism of chaperonin-fibril interaction. Initial fibril solution is heterogeneous and is composed of several fibril polymorphs (gray and colored). We found that one of them (colored) is resistant to the chaperonins activity. At the same time, another polymorph architecture is ruined, after chaperonins (blue circles) bind to its surface and melt fibril β-sheet structure. As a result of chaperonin's activity fibrils break down, swell and coagulate forming large gelatinous aggregates (shown by gray). (For interpretation of the references to color in this figure legend, the reader is referred to the web version of this article.)

disaggregate $(A\beta)_{1-40}$ and the 8 kDa plasma gelsolin fragment fibrils. They found that the disaggregation cocktail is sensitive to proteinase K digestion. Based on these results they concluded that proteins rather than small molecules are responsible for amyloid degradation. It is known that various chaperones and chaperonins are highly expressed components of cells, whose main function is a cooperative protein folding. Our results indicate that chaperonins have high fibril disaggregation activity. It is tempting to speculate that the components responsible for fibril disaggregation, previously observed by Kelly and co-workers [32] in cell extracts, are chaperonins.

Summarizing, our results establish that an ATP-dependant Cpn can degrade amyloid fibrils under mild conditions. We found that Cpn bound to fibrils and rapidly modified their architecture under mild conditions. As a result, insulin fibrils became large gelatinous aggregates. We anticipate these results will initiate broader studies, involving other Cpn and chaperone combinations to not only degrade fibrils, but also to refold the proteins and restore normal biological activity as the final result of the process.

Acknowledgments

We thank Dr. Ilya Baskakov for helpful discussion. Dr. Shekhtman and Jacqueline Washington for the help with free protein detection. Maruda Shanmugasundaram for helpful advice. This research was Funded by the Air Force Office of Scientific Research Air Force Grants AFOSR 03-S-28900, 9550-10-1-0272 and National Science Foundation Grant CHE-1152752.

Appendix A. Supplementary data

Supplementary data associated with this article can be found, in the online version, at http://dx.doi.org/10.1016/j.bbrc.2012.04.113.

References

[1] S. Treusch, D.M. Cyr, S. Lindquist, Amyloid deposits: protection against toxic protein species?, Cell Cycle 8 (2009) 1668–1674

[2] H. Kim, B.S. Park, K.G. Lee, C.Y. Choi, S.S. Jang, Y.H. Kim, S.E. Lee, Effects of naturally occurring compounds on fibril formation and oxidative stress of beta-amyloid, J. Agric. Food Chem 53 (2005) 8537–8541.

[3] G. Bomhoff, K. Sloan, C. McLain, E.P. Gogol, M.T. Fisher, The effects of the flavonoid baicalein and osmolytes on the Mg^{2+} accelerated aggregation/fibrillation of carboxymethylated bovine 1SS-alpha-lactalbumin, Arch. Biochem. Biophys. 453 (2006) 75–86.

[4] J. Brange, L. Andersen, E.D. Laursen, G. Meyn, E. Rasmussen, Toward understanding insulin fibrillation, J. Pharm. Sci. 86 (1997) 517–525.

[5] H.Y. Kim, M.K. Cho, D. Riedel, C.O. Fernandez, M. Zweckstetter, Dissociation of amyloid fibrils of alpha-synuclein in supercooled water, Angew Chem Int Ed Engl 47 (2008) 5046–5048.

[6] S. Baglioni, F. Casamenti, M. Bucciantini, L.M. Luheshi, N. Taddei, F. Chiti, C.M. Dobson, M. Stefani, Prefibrillar amyloid aggregates could be generic toxins in higher organisms, J. Neurosci. 26 (2006) 8160–8167.

[7] M. Bucciantini, E. Giannoni, F. Chiti, F. Baroni, L. Formigli, J. Zurdo, N. Taddei, G. Ramponi, C.M. Dobson, M. Stefani, Inherent toxicity of aggregates implies a common mechanism for protein misfolding diseases, Nature 416 (2002) 507–511.

[8] T. Zako, M. Sakono, N. Hashimoto, M. Ihara, M. Maeda, Bovine insulin filaments induced by reducing disulfide bonds show a different morphology, secondary structure, and cell toxicity from intact insulin amyloid fibrils, Biophys. J. 96 (2009) 3331–3340.

[9] F.E. Dische, C. Wernstedt, G.T. Westermark, P. Westermark, M.B. Pepys, J.A. Rennie, S.G. Gilbey, P.J. Watkins, Insulin as an amyloid-fibril protein at sites of repeated insulin injections in a diabetic patient, Diabetologia 31 (1988) 158–161.

[10] S. Storkel, H.M. Schneider, H. Muntefering, S. Kashiwagi, Iatrogenic, insulin-dependent, local amyloidosis, Lab. Invest. 48 (1983) 108–111.

[11] D. Kurouski, R.A. Lombardi, R.K. Dukor, I.K. Lednev, L.A. Nafie, Direct observation and pH control of reversed supramolecular chirality in insulin fibrils by vibrational circular dichroism, Chem. Commun. 46 (2010) 7154–7156.

[12] M.M. Wilhelmus, W.C. Boelens, I. Otte-Holler, B. Kamps, R.M. de Waal, M.M. Verbeek, Small heat shock proteins inhibit amyloid-beta protein aggregation and cerebrovascular amyloid-beta protein toxicity, Brain Res. 1089 (2006) 67–78.

[13] B. Raman, T. Ban, M. Sakai, S.Y. Pasta, T. Ramakrishna, H. Naiki, Y. Goto, M. Rao Ch, AlphaB-crystallin, a small heat-shock protein, prevents the amyloid fibril growth of an amyloid beta-peptide and beta2-microglobulin, Biochem. J. 392 (2005) 573–581.

[14] H. Ecroyd, J.A. Carver, Crystallin proteins and amyloid fibrils, Cell Mol. Life Sci. 66 (2009) 62–81.

[15] Y.H. Liu, Y.L. Han, J. Song, Y. Wang, Y.Y. Jing, Q. Shi, C. Tian, Z.Y. Wang, C.P. Li, J. Han, X.P. Dong, Heat shock protein 104 inhibited the fibrillization of prion peptide 106–126 and disassembled prion peptide 106–126 fibrils in vitro, Int. J. Biochem. Cell Biol. 43 (2011) 768–774.

[16] M. Arimon, V. Grimminger, F. Sanz, H.A. Lashuel, Hsp104 targets multiple intermediates on the amyloid pathway and suppresses the seeding capacity of Abeta fibrils protofibrils, J. Mol. Biol. 384 (2008) 1157–1173.

[17] C.A. Waudby, T.P. Knowles, G.L. Devlin, J.N. Skepper, H. Ecroyd, J.A. Carver, M.E. Welland, J. Christodoulou, C.M. Dobson, S. Meehan, The interaction of alphaB-crystallin with mature alpha-synuclein amyloid fibrils inhibits their elongation, Biophys. J. 98 (2010) 843–851.

[18] Y. Sun, N. Makarava, C.I. Lee, P. Laksanalamai, F.T. Robb, I.V. Baskakov, Conformational stability of PrP amyloid fibrils controls their smallest possible fragment size, J. Mol. Biol. 376 (2008) 1155–1167.
[19] C. Behrends, C.A. Langer, R. Boteva, U.M. Bottcher, M.J. Stemp, G. Schaffar, B.V. Rao, A. Giese, H. Kretzschmar, K. Siegers, F.U. Hartl, Chaperonin TRiC promotes the assembly of polyQ expansion proteins into nontoxic oligomers, Mol. Cell 23 (2006) 887–897.
[20] K.C. Luk, I.P. Mills, J.Q. Trojanowski, V.M. Lee, Interactions between Hsp70 and the hydrophobic core of alpha-synuclein inhibit fibril assembly, Biochemistry 47 (2008) 12614–12625.
[21] M.M. Dedmon, J. Christodoulou, M.R. Wilson, C.M. Dobson, Heat shock protein 70 inhibits alpha-synuclein fibril formation via preferential binding to prefibrillar species, J. Biol. Chem. 280 (2005) 14733–14740.
[22] S.F. Falsone, A.J. Kungl, A. Rek, R. Cappai, K. Zangger, The molecular chaperone Hsp90 modulates intermediate steps of amyloid assembly of the Parkinson-related protein alpha-synuclein, J. Biol. Chem. 284 (2009) 31190–31199.
[23] C. Huang, H. Cheng, S. Hao, H. Zhou, X. Zhang, J. Gao, Q.H. Sun, H. Hu, C.C. Wang, Heat shock protein 70 inhibits alpha-synuclein fibril formation via interactions with diverse intermediates, J. Mol. Biol. 364 (2006) 323–336.
[24] H. Luo, P. Laksanalamai, F.T. Robb, An exceptionally stable Group II chaperonin from the hyperthermophile *Pyrococcus furiosus*, Arch. Biochem. Biophys. 486 (2009) 12–18.
[25] H. Kubota, G. Hynes, K. Willison, The chaperonin containing t-complex polypeptide 1 (TCP-1). Multisubunit machinery assisting in protein folding and assembly in the eukaryotic cytosol, Eur. J. Biochem. 230 (1995) 3–16.
[26] P. Laksanalamai, F.T. Robb, Small heat shock proteins from extremophiles: a review, Extremophiles 8 (2004) 1–11.
[27] F.T. Robb, D.L. Maeder, J.R. Brown, J. DiRuggiero, M.D. Stump, R.K. Yeh, R.B. Weiss, D.M. Dunn, Genomic sequence of hyperthermophile, *Pyrococcus furiosus*: implications for physiology and enzymology, Methods Enzymol. 330 (2001) 134–157.
[28] H. Luo, F.T. Robb, A modulator domain controlling thermal stability in the Group II chaperonins of Archaea, Arch. Biochem. Biophys. 512 (2011) 111–118.
[29] T.P. Knowles, D.A. White, A.R. Abate, J.J. Agresti, S.I. Cohen, R.A. Sperling, E.J. De Genst, C.M. Dobson, D.A. Weitz, Observation of spatial propagation of amyloid assembly from single nuclei, Proc. Natl. Acad. Sci. USA 108 (2011) 14746–14751.
[30] S.M. Techtmann, F.T. Robb, Archaeal-like chaperonins in bacteria, Proc. Natl. Acad. Sci. USA 107 (2010) 20269–20274.
[31] J.L. Jimenez, E.J. Nettleton, M. Bouchard, C.V. Robinson, C.M. Dobson, H.R. Saibil, The protofilament structure of insulin amyloid fibrils, Proc. Natl. Acad. Sci. USA 99 (2002) 9196–9201.
[32] A.N. Murray, J.P. Solomon, Y.J. Wang, W.E. Balch, J.W. Kelly, Discovery and characterization of a mammalian amyloid disaggregation activity, Protein Sci. 19 (2010) 836–846.